Published in final edited form as:

Eur Radiol. 2022 February ; 32(2): 1308–1319. doi:10.1007/s00330-021-08235-8.

T_1 and T_2 quantification using magnetic resonance fingerprinting in mild traumatic brain injury

Teresa Gerhalter[1], **Martijn Cloos**[1,2], **Anna M. Chen**[1], **Seena Dehkharghani**[1,3], **Rosemary Peralta**[1], **James S. Babb**[1], **Alejandro Zarate**[4], **Tamara Bushnik**[4], **Jonathan M. Silver**[5], **Brian S. Im**[4], **Stephen Wall**[6], **Steven Baete**[1,7], **Guillaume Madelin**[1], **Ivan I. Kirov**[1,3,7]

[1]Center for Biomedical Imaging, Department of Radiology, New York University Grossman School of Medicine, New York, NY, USA

[2]Centre for Advanced Imaging, The University of Queensland, Brisbane, Australia

[3]Department of Neurology, New York University Grossman School of Medicine, New York, NY, USA

[4]Department of Rehabilitation Medicine, New York University Grossman School of Medicine, New York, NY, USA

[5]Department of Psychiatry, New York University Grossman School of Medicine, New York, NY, USA

[6]Ronald O. Perelman Department of Emergency Medicine, New York University Grossman School of Medicine, New York, NY, USA

[7]Center for Advanced Imaging Innovation and Research, Department of Radiology, New York University Grossman School of Medicine, 660 First Avenue, New York, NY, USA

Abstract

✉Guillaume Madelin, guillaume.madelin@nyulangone.org; Ivan I. Kirov, ivan.kirov@nyulangone.org.

Supplementary Information The online version contains supplementary material available at https://doi.org/10.1007/s00330-021-08235-8.

Guarantor The scientific guarantor of this publication is Ivan Kirov, Ph.D.

Conflict of interest The authors of this manuscript declare no relationships with any companies whose products or services may be related to the subject matter of the article.

Statistics and biometry One of the authors has significant statistical expertise (James Babb, Ph.D.).

Informed consent Written informed consent was obtained from all subjects in this study.

Ethical approval Institutional Review Board approval was obtained for this study.

Study subjects or cohorts overlap The subject cohorts have been previously reported on in the following publication: Gerhalter et al, Global decrease in brain sodium concentration after mild traumatic brain injury. Brain Communications, Volume 3, Issue 2, 2021, https://doi.org/10.1093/braincomms/fcab051.
The overlap is mentioned in the manuscript and the details are thoroughly described in the Supplemental Materials section.
Methodology
• prospective
• cross-sectional study/diagnostic or prognostic study.
• performed at one institution.

Objectives—To assess whether MR fingerprinting (MRF)–based relaxation properties exhibit cross-sectional and prospective correlations with patient outcome and compare the results with those from DTI.

Methods—Clinical imaging, MRF, and DTI were acquired in patients (24 ± 10 days after injury (timepoint 1) and 90 ± 17 days after injury (timepoint 2)) and once in controls. Patient outcome was assessed with global functioning, symptom profile, and neuropsychological testing. ADC and fractional anisotropy (FA) from DTI and T_1 and T_2 from MRF were compared in 12 gray and white matter regions with Mann–Whitney tests. Bivariate associations between MR measures and outcome were assessed using the Spearman correlation and logistic regression.

Results—Data from 22 patients (38 ± 12 years; 17 women) and 18 controls (32 ± 8 years; 12 women) were analyzed. Fourteen patients (37 ± 12 years; 11 women) returned for timepoint 2, while two patients provided only timepoint 2 clinical outcome data. At timepoint 1, there were no differences between patients and controls in T_1, T_2, and ADC, while FA was lower in mTBI frontal white matter. T_1 at timepoint 1 and the change in T_1 exhibited more (n = 18) moderate to strong correlations ($|r|$= 0.6–0.85) with clinical outcome at timepoint 2 than T_2 (n = 3), FA (n = 7), and ADC (n = 2). High T_1 at timepoint 1, and serially increasing T_1, accounted for five of the six MR measures with the highest utility for identification of non-recovered patients at timepoint 2 (AUC > 0.80).

Conclusion—T_1 derived from MRF was found to have higher utility than T_2, FA, and ADC for predicting 3-month outcome after mTBI.

Keywords

Traumatic brain injury; Magnetic resonance fingerprinting; Relaxation; Clinical outcome

Introduction

Mild traumatic brain injury (mTBI) is a leading public health problem in civilian, as well as in military veteran, populations, amounting to an annual worldwide incidence of ~ 55 million [1, 2]. Although most patients recover completely, a subset develops persistent physical, psychiatric, emotional, or cognitive impairments [3]. Because their brain CT and qualitative MRI are most commonly negative [4, 5], there is a need for quantitative imaging-based markers to improve mTBI prognosis.

Diffuse axonal injury is thought to be the pathological process behind most TBI-related impairments [6]. Ionic imbalances cause axonal varicosities and other micro-structural damage to axonal tracts, which has been commonly studied using diffusion tensor imaging (DTI) [7, 8]. However, DTI findings are highly variable with respect to anatomical location, nature of alterations, and their correlation with clinical outcome [9]. Thus, there is a need for additional non-invasive markers that are sensitive to diffuse axonal injury and its related cellular changes. Changes in the local molecular environment of water are detectable with quantitative assessment of its longitudinal (T_1) and transverse (T_2) relaxation times, but despite promising results from TBI animal models [10–12], human studies are lacking. The only two in vivo investigations reported higher T_2 in patients with predominantly moderate and severe TBI [13, 14]; while a recent ex vivo study linked T_1 and T_2 to diffuse axonal

injury [15]. Further research has likely been hampered by the fact that most relaxometry approaches require long acquisition times limited to only a single property (T_1 or T_2). Fortunately, clinical applications of quantitative relaxometry have been made possible by magnetic resonance fingerprinting (MRF) [16], which enables fast reconstruction of different parameters from a single MRI acquisition [17, 18].

Given that (*i*) diffuse axonal injury is expected to change the molecular environment of water; and (*ii*) the previous animal studies [11, 12] in TBI found relaxation time increases correlating with outcomes, we hypothesized that higher relaxation times will be detectable in vivo by MRF in mTBI and that they will show cross-sectional and prospective correlations with patient outcome. These hypotheses were tested in gray matter (GM) and white matter (WM) regions of patients scanned at an average of 24 days after TBI (timepoint 1) and subsequently at a three-month follow-up (timepoint 2). The aims were to assess whether MRF-based relaxation properties (T_1, T_2) exhibit correlations with patient outcome and to compare the results to those obtained with the established DTI metrics of fractional anisotropy (FA) and apparent diffusion coefficient (ADC).

Methods

Study participants

The Institutional Review Board approved this Health Insurance Portability and Accountability Act–compliant study, and informed written consent was obtained prior to the examination. Between November 2018 and December 2019, we prospectively enrolled 31 patients (23 women, average age 37 ± 12 years) with mTBI to be scanned at an average of 1 month after injury, with a follow-up visit at an average 3 months after injury (Fig. 1). The inclusion criteria besides diagnosis of mTBI [19], along with exclusion criteria, are listed in the Supplemental Materials. Eighteen age- and sex-matched healthy volunteers (12 women, average age 32 ± 8 years) were included as controls and scanned once. This patient and control cohort is being studied with multimodal and multinuclear MRI as part of a larger project, which, at the time of publication, has produced one other manuscript [20]. Specific areas of data overlap between the two publications are reported in the Supplemental Materials.

Patient outcome assessment

At the time of each MRI visit, patients underwent clinical and neuropsychological assessment using the following tools from the National Institute of Neurological Disorders and Stroke TBI Common Data Elements database: the Rivermead Post-Concussion Symptoms Questionnaire (RPQ) [21], which inquires about 16 symptoms frequently reported after mTBI; the Glasgow Outcome Scale – Extended (GOSE) [22], to assess the impact of an injury on daily life function; and the Brief Test of Adult Cognition by Telephone (BTACT) [23], to evaluate memory and executive functioning using performance-based cognitive testing. All assessments were performed by the research coordinator, who was unaware of any individual's MRI data or results.

MRI acquisition

Imaging was performed on a 3-T scanner (Magnetom Prisma, Siemens Healthineers). The qualitative MRI protocol consisted of a 2D fluid-attenuation inversion recovery, a 3D T_1-weighted gradient echo, and susceptibility-weighted imaging. DTI was acquired with a mono-polar gradient pulse echo-planar imaging sequence (nine b_0 images with $b = 250$, 1000, and 2000s/mm^2). For multiparametric mapping, we applied a multi-slice 2D radial MRF method to simultaneously measure T_1 and T_2, as previously described [24], with the following parameters: in-plane resolution of 1.25 × 1.25 mm^2, 5-mm slice thickness, and a total scan time of less than 8 min. A dictionary with simulated MR fingerprints was created using extended-phase graphs with T_1 and T_2 entries in the ranges 150–4642 ms and 10–350 ms, respectively (step size of 2.5%) [24]. Imaging parameter details are provided in Table A.1 in the Supplemental Materials.

Image analysis

Qualitative images were evaluated by a neuroradiologist using the NIH Common Data Element guidelines [25]. MRI findings were manually outlined and excluded from the quantitative analysis to investigate only normal-appearing tissue. Twelve regions known for susceptibility to TBI and that are common sites of DTI abnormalities [25, 26] were extracted from the T_1-weighted images to obtain average regional values of T_1, T_2, FA, and ADC (Fig. 2). Automatic brain segmentation was performed using FreeSurfer version 6.0.0 [27] to obtain global WM, global cortical GM, and four deep GM masks. Six regional WM masks were manually outlined using FireVoxel software [28, 29]. The global cortical GM and thalamus masks were eroded by one voxel, to reduce partial volume errors from neighboring cerebrospinal fluid.

Post-processing of diffusion data was performed offline using software tools from FSL [30] and MRTrix3.0 [31] to generate ADC and FA maps for each voxel. The MRF data was reconstructed offline with an in-house MATLAB script. Visual quality control ensured that only artifact-free slices were included in the analysis [32]. Slices with motion artifacts were completely excluded from the ROI analysis.

All outlined regions were individually registered to the DTI and MRF maps in SPM12. The ROIs were overlaid on the maps, and voxel values within each ROI were averaged. To account for partial volume effects, voxels with a cerebrospinal fluid fraction greater than 0.3 were excluded from the analysis. For the estimation of the relaxation times, outliers defined by $T_1 > 2500$ ms and $T_2 > 150$ ms were also excluded (average ± two standard deviations of T_1/T_2 of cerebrospinal fluid).

All data analyses, including the radiologist’s readings, were done blinded to the patient’s clinical outcome data.

Statistical analysis

Sample size and statistical power calculations were performed as described in the Supplemental Materials. Nonparametric analyses were conducted due to their robustness against violations of the assumption of normality. The Mann–Whitney test was used to

compare the control to the mTBI group. Since the T_1 and T_2 relationships with age are not well-characterized, the three oldest patients (ages 56, 59, and 60 years), who lacked age-matched controls, were omitted from the intergroup analyses comparing patients and controls but were included in the mTBI intragroup analyses (see Supplemental Materials). Bivariate associations were assessed using the nonparametric Spearman rank correlation. Logistic regression was used to identify measures that could discriminate patients who were recovered at timepoint 2 (GOSE = 8), from those who were not (GOSE < 8). The area under the receiver-operating-characteristic curve (AUC) assessed the performance of each imaging measure at timepoint 1 as a predictor of recovery. All statistical tests were conducted at the two-sided 5% significance level using SAS 9.4 software (SAS Institute, USA). *p* values are reported without multiple comparison corrections due to the exploratory nature of this study.

Results

Study population

Out of the 31 patients who signed informed consent, 22 contributed data at timepoint 1, 16 of which returned for a scan at timepoint 2. Reasons for exclusion or drop-out are shown in Fig. 1. Table 1 details the demographic and injury characteristics of the patients used in the analysis. The average time from injury at timepoint 1 was 24 ± 10 (average ± standard deviation) days (range: 8–53), and 90 ± 17 days (range: 82–142) at timepoint 2. Two patients scanned at timepoint 1 declined a scan at timepoint 2, but responded to the outcome questionnaires over the phone at 115 and 113 days after injury. Hemorrhagic diffuse axonal injury and non-axonal shear patterns of hemorrhages were observed on qualitative MRI in two patients.

Patient outcome assessments

Results of the outcome assessments are compiled in Table 2. RPQ data was analyzed according to three classifications: (*i*) RPQ total score [21]; (*ii*) RPQ 3 and RPQ 13, which groups early- and late-onset symptoms, respectively [33]; and (*iii*) three-factor model with cognitive, somatic, and emotional subscales [34]. Concussion symptoms using all three RPQ methods improved over time (all $p < 0.05$), as did the GOSE ($p = 0.005$). Two BTACT subtests, namely word list recall ($p = 0.005$) and number series ($p = 0.005$), as well as the composite BTACT z-score ($p = 0.001$) improved over time, indicating improvement of memory and executive functioning.

Quantitative MRI measures at timepoint 1

Figure 3 shows example T_1, T_2, ADC, and FA maps next to qualitative images from a patient and an age-matched control. In general, GM exhibited higher T_1 and T_2 values than WM, producing high gray-white matter contrast. Figure 4 shows the distributions of T_1, T_2, ADC, and FA in all ROIs in patients and controls at timepoint 1. Numerical values are provided in Table A.2 and A.3. FA in frontal WM was lower in mTBI compared to controls ($p = 0.017$). There were no statistically significant differences in T_1 and T_2 between patients and controls at timepoint 1 (Table A.4).

Quantitative MRI measures at timepoint 2 and changes compared to timepoint 1

At timepoint 2, ADC and T_1 in caudate and in global cortical GM were lower in mTBI compared to controls (all $p < 0.05$) (Table A.4). Statistically significant within-subject changes (value at timepoint 2 minus the value at timepoint 1, Δ 2–1) in MRI measures among patients who provided data at both timepoints are compiled in Table 3. FA in the body of the corpus callosum, corona radiata, thalamus, and global cortical GM dropped over time, while the T_2 in the pallidum increased (all $p < 0.05$).

Cross-sectional relationships between MRI measures and patient outcome

All statistically significant correlations are presented in Tables A.5 and A.6, while a graphical summary of those for MRF is shown in Fig. 5.

At timepoint 1, the number of correlations and their average strength were similar amongst all MRI metrics (Table A.5). At timepoint 2, T_1 showed the largest number of correlations, but their average strength was comparable to that of DTI (Table A.6). All MRI measures showed higher number, and stronger correlations with clinical outcome at timepoint 2, than at timepoint 1 (Table A.5 vs A.6).

While there was the same amount of T_2 correlations at both timepoints, there were almost eight times more correlations for T_1 at timepoint 2, compared to timepoint 1 (Fig. 5a). T_1 and T_2 correlated with the RPQ at both timepoints, and with the GOSE only at the second timepoint. Correlations with the BTACT were detected with T_2 at timepoint 1, and with T_1 at timepoint 2 (Fig. 5a). Apart from RPQ at timepoint 1, the directionality of these associations was consistent (Fig. 5b). Both relaxation times showed stronger associations with clinical measures at timepoint 2 than at timepoint 1 (Fig. 5c). The strongest associations ($r > |0.7|$) were between genu T_1 and RPQ (Table A.6).

Predictive relationships between MRI measures and patient clinical outcome

The statistically significant correlations between MRI values at timepoint 1 and clinical outcome at timepoint 2, as well as those between the longitudinal change in MRI values (Δ 2–1) and clinical outcome at timepoint 2, are compiled in Table A.7. A graphical summary of the MRF correlations is shown in Fig. 5.

There were six times more correlations between T_1 at timepoint 1 and clinical outcomes at timepoint 2, than between T_2 at timepoint 1 and clinical outcomes at timepoint 2 (Fig. 5a). The longitudinal change in T_1 showed two times more correlations with clinical outcome at timepoint 2, compared to the longitudinal change in T_2 (Fig. 5a). Correlations with RPQ were dominant in the comparisons between the longitudinal change of relaxation times and clinical outcome at timepoint 2, while correlations with the BTACT were dominant in the comparisons between relaxation times at timepoint 1 and clinical outcome at timepoint 2 (Fig. 5a). The directionality of these associations was consistent: positive for RPQ and BTACT, and negative for GOSE (Fig. 5b). As shown in Fig. 5c, predictive relationships between MRF and clinical outcome were stronger for T_1.

T_1 showed the largest number of both types of correlations, and their average strength across all outcome measures was always higher than that of DTI (Table A.7). Out of the four strongest associations of any metric three were for genu T_1 (Fig. 6).

Patients were dichotomized according to their GOSE at timepoint 2 to recovered ($n = 8$) or non-recovered ($n = 11$). As shown in Table 4, the following measures obtained at timepoint 1 were found to be good discriminators (defined as AUC > 0.80) between recovered and non-recovered individuals at timepoint 2: T_1 of the corona radiata, posterior WM, and splenium, as well as ADC of the corona radiata. The change from timepoint 1 to timepoint 2 as a predictor of recovery at timepoint 2 was a good discriminator for the T_1 of the frontal WM and the genu.

Discussion

Pre-clinical and limited human data suggest that quantification of relaxation times is a promising marker for TBI pathology and clinical outcomes. Here we evaluated the potential of quantitative T_1 and T_2 to predict patient outcome following mTBI. The major findings were as follows. MRF differences between patients and controls were absent at timepoint 1 and were limited at timepoint 2 to two regions of abnormal T_1. DTI differences were found at the same frequency at timepoint 2 (two regions with abnormal ADC), while at timepoint 1, one region showed a difference in FA. The cross-sectional correlations of T_1 and T_2 with clinical outcome were similar in number and strength to those observed with DTI. However, both T_1 at timepoint 1 and the serial change in T_1 revealed more and stronger predictive correlations with clinical outcome 3 months after injury than did T_2, ADC, or FA. Moreover, T_1 of five regions enabled the identification of non-recovered patients at the follow-up visit with AUC > 0.80. ADC showed one association in the same AUC range, while T_2 and FA showed none. There are three notable aspects of these predictive properties. First, they arose from T_1 values, while T_2 performed on par with DTI. Second, higher or serially increasing relaxation times were consistently linked to worse global functional (GOSE) and symptomatology (RPQ) outcome; the association of relaxation times with neuropsychological testing (BTACT) scores was clear only for T_1, with low values linked to a worse score. Third, the prediction was largely related to relaxation times originating from WM, as expected given the putative effects of diffuse axonal injury in post-concussive symptomatology. T_1 of the genu showed some of the strongest cross-sectional and predictive correlations with RPQ and BTACT, and a high AUC for the GOSE-defined outcome.

Our focus on the relaxation properties of water stems from previous work showing that they can be affected by cytoskeletal damage, inflammation, and edema [35, 36]. T_1 and T_2 relaxation depend on the concentration of macromolecules and the level of binding between them and water. Specifically, water protons in the vicinity of macromolecules have short T_1 and T_2 [37]. Previous pre-clinical studies [10–12] reported elevated T_2, which was explained by vasogenic edema. In addition, elevated $T_1\rho$ and T_2 following resolution of edema were predictive of long-term outcome, possibly due to progressive neuronal loss [11]. The two previous investigations in human TBI also reported elevated T_2, including in normal-appearing WM [13, 14]. Our study did not find conclusive evidence for altered relaxation times in normal-appearing tissue, but our cohort consisted only of mTBI patients, while the

previous studies consisted of mostly moderate and severe TBI [13, 14]. Importantly, while the prior literature reports change exclusively in T_2, we found stronger correlations with clinical outcome for T_1. The directionality of these associations was consistent, with higher, or increasing values associated with worse outcome in symptoms and global functioning, and lower values associated with worse neuropsychological testing scores. The question therefore arises, whether, similarly to FA, higher and lower relaxation values reflect different pathologies, which in turn can be linked to different functional domains. Conjecturing any further based on our data, however, including as to what biological processes higher and lower values may represent, is speculative, especially given the lack of convincing evidence that relaxation times are altered compared to controls.

The results must be viewed in the context of the following limitations. First, multiple comparison corrections were not performed. Due to the lack of previous relaxation time studies in mTBI, this project qualified as exploratory, and therefore, we aimed to uncover the most true findings, with the understanding that type I errors were not controlled, and the results require replication. We therefore report on overall trends and avoid giving disproportionate weight to individual findings. Our statistical approach, however, may not be appropriate for DTI, given the vast body of prior literature. Therefore, we use the DTI results solely for comparison to MRF and refrain from comparing them to past DTI studies. Second, DTI did not show widespread changes, and only two patients had findings on qualitative MR images. It is possible that MRF shows better utility in differentiating controls from patients who show more macro- and micro-structural injury. Third, SWI at 7 T would be better suited to answer the question of whether relaxation times are related to subtle micro-bleeds, which are more readily identified at ultra-high field [38, 39]. As more 7 T systems become available for clinical use, quantitative MR modalities, such as MRF, should also be utilized in TBI to test whether they show increased sensitivity. Fourth, scanning occurred within a wide range of time around the 1- and 3-month timepoints. The pathological process post-TBI is dynamic [40], which could have potentially decreased the sensitivity of MRF and DTI. Finally, the findings of this study should be interpreted in the context of the study design, the patient population, and the limited sample size. The findings that MRF is prognostically better than DTI needs further validation on a larger population.

Conclusion

MRF-based relaxometry, which enables collection of water relaxation times within clinical scan timeframes, revealed no widespread differences in T_1 and T_2 between patients and controls at 1 and at 3 months post-mTBI. However, WM T_1 at 1 month and the change of WM T_1 from 1 to 3 months were linked to clinical and neurocognitive impairments at 3 months after injury. These correlations were stronger than those for T_2 and stronger than those for FA and ADC from DTI and motivate studies to determine whether MRF can provide a differential increase in prognostic accuracy beyond qualitative MRI and DTI.

Supplementary Material

Refer to Web version on PubMed Central for supplementary material.

Acknowledgements

We thank all participants for their time and interest in this study.

Funding

This study has received funding by the United States' National Institutes of Health (NIH) through grants numbers R01NS097494 and R01EB026456.

Abbreviations

BTACT	Brief Test of Adult Cognition by Telephone
DTI	Diffusion tensor imaging
GM	Gray matter
GOSE	Glasgow outcome scale – extended
MRF	Magnetic resonance fingerprinting
mTBI	Mild traumatic brain injury
RPQ	Rivermead post-concussion symptoms questionnaire
T_1	Longitudinal relaxation times
T_2	Transverse relaxation times
WM	White matter

References

1. Dang B, Chen W, He W, Chen G (2017) Rehabilitation treatment and progress of traumatic brain injury dysfunction. Neural Plast 2017:1–6. 10.1155/2017/1582182
2. Beran R, Bhaskar S (2018) Concussion within the military. J Mil Veterans Health 26:20–27
3. Maas AIR, Menon DK, Adelson PD et al. (2017) Traumatic brain injury: integrated approaches to improve prevention, clinical care, and research. Lancet Neurol 16:987–1048. 10.1016/S1474-4422(17)30371-X [PubMed: 29122524]
4. Wang KK, Yang Z, Zhu T et al. (2018) An update on diagnostic and prognostic biomarkers for traumatic brain injury. Expert Rev Mol Diagn 18:165–180. 10.1080/14737159.2018.1428089 [PubMed: 29338452]
5. Blennow K, Brody DL, Kochanek PM et al. (2016) Traumatic brain injuries. Nat Rev Dis Prim 2:16084. 10.1038/nrdp.2016.84 [PubMed: 27853132]
6. Bešsenski N (2002) Traumatic injuries: imaging of head injuries. Eur Radiol 12:1237–1252. 10.1007/s00330-002-1355-9 [PubMed: 12042929]
7. Shenton ME, Hamoda HM, Schneiderman JS et al. (2012) A review of magnetic resonance imaging and diffusion tensor imaging findings in mild traumatic brain injury. Brain Imaging Behav 6:137–192. 10.1007/sll682-012-9156-5 [PubMed: 22438191]
8. Hergan K, Schaefer P, Sorensen A et al. (2002) Diffusion-weighted MRI in diffuse axonal injury of the brain. Eur Radiol 12:2536–2541. 10.1007/s00330-002-1333-2 [PubMed: 12271396]
9. Wallace EJ, Mathias JL, Ward L (2018) The relationship between diffusion tensor imaging findings and cognitive outcomes following adult traumatic brain injury: a meta-analysis. Neurosci Biobehav Rev 92:93–103. 10.1016/j.neubiorev.2018.05.023 [PubMed: 29803527]

10. Li W, Watts L, Long J et al. (2016) Spatiotemporal changes in blood-brain barrier permeability, cerebral blood flow, T2 and diffusion following mild traumatic brain injury. Brain Res 1646:53–61. 10.1016/j.brainres.2016.05.036 [PubMed: 27208495]
11. Immonen RJ, Kharatishvili I, Gröhn H et al. (2009) Quantitative MRI predicts long-term structural and functional outcome after experimental traumatic brain injury. Neuroimage 45:1–9. 10.1016/j.neuroimage.2008.11.022 [PubMed: 19101638]
12. Kharatishvili I, Sierra A, Immonen RJ et al. (2009) Quantitative T2 mapping as a potential marker for the initial assessment of the severity of damage after traumatic brain injury in rat. Exp Neurol 217:154–164. 10.1016/j.expneurol.2009.01.026 [PubMed: 19416663]
13. Kumar R, Gupta RK, Rao SB et al. (2003) Magnetization transfer and T2 quantitation in normal appearing cortical gray matter and white matter adjacent to focal abnormality in patients with traumatic brain injury. Magn Reson Imaging 21:893–899. 10.1016/S0730-725X(03)00189-9 [PubMed: 14599540]
14. Mamere AE, Saraiva LAL, Matos ALM et al. (2009) Evaluation of delayed neuronal and axonal damage secondary to moderate and severe traumatic brain injury using quantitative MR imaging techniques. Am J Neuroradiol 30:947–952. 10.3174/ajnr.A1477 [PubMed: 19193759]
15. Benjamini D, Iacono D, Komlosh ME et al. (2021) Diffuse axonal injury has a characteristic multidimensional MRI signature in the human brain. Brain 144:800–816. 10.1093/brain/awaa447 [PubMed: 33739417]
16. Ma D, Gulani V, Seiberlich N et al. (2013) Magnetic resonance fingerprinting. Nature 495:187–192. 10.1038/naturell971 [PubMed: 23486058]
17. Badve C, Yu A, Dastmalchian S et al. (2017) MR fingerprinting of adult brain tumors: initial experience. Am J Neuroradiol 38:492–499. 10.3174/ajnr.A5035
18. Keil VC, Bakoeva SP, Jurcoane A et al. (2019) MR fingerprinting as a diagnostic tool in patients with frontotemporal lobe degeneration: a pilot study. NMR Biomed 32:1–13. 10.1002/nbm.4157
19. Kay T, Harrington DE, Adams R (1993) American Congress of Rehabilitation Medicine, Head Injury Interdisciplinary Special Interest Group. Definition of mild traumatic brain injury. J Head Trauma Rehabil 8:86–87
20. Gerhalter T, Chen AM, Dehkharghani S et al. (2021) Global decrease in brain sodium concentration after mild traumatic brain injury. Brain Commun 3. 10.1093/braincomms/fcab051
21. King NS, Crawford S, Wenden FJ et al. (1995) The Rivermead Post Concussion Symptoms Questionnaire: a measure of symptoms commonly experienced after head injury and its reliability. J Neurol 242:587–592. 10.1007/BF00868811 [PubMed: 8551320]
22. Wilson JT, Pettigrew LE, Teasdale GM (1998) Structured interviews for the Glasgow Outcome Scale and the extended Glasgow Outcome Scale: guidelines for their use. J Neurotrauma 15:573–585. 10.1089/neu.1998.15.573 [PubMed: 9726257]
23. Tun PA, Lachman ME (2006) Telephone assessment of cognitive function in adulthood: the Brief Test of Adult Cognition by Telephone. Age Ageing 35:629–632. 10.1093/ageing/af1095 [PubMed: 16943264]
24. Cloos MA, Assländer J, Abbas B et al. (2019) Rapid Radial T1 and T2 Mapping of the Hip Articular Cartilage With Magnetic Resonance Fingerprinting. J Magn Reson Imaging 50:810–815. 10.1002/jmri.26615 [PubMed: 30584691]
25. Haacke EM, Duhaime AC, Gean AD et al. (2010) Common data elements in radiologic imaging of traumatic brain injury. J Magn Reson Imaging 32:516–543. 10.1002/jmri.22259 [PubMed: 20815050]
26. Hulkower MB, Poliak DB, Rosenbaum SB et al. (2013) A decade of DTI in traumatic brain injury: 10 years and 100 articles later. Am J Neuroradiol 34:2064–2074. 10.3174/ajnr.A3395 [PubMed: 23306011]
27. Fischl B (2012) FreeSurfer. Neuroimage 62:774–781. 10.1016/j.neuroimage.2012.01.021 [PubMed: 22248573]
28. Rusinek H, Glodzik L, Mikheev A et al. (2013) Fully automatic segmentation of white matter lesions: error analysis and validation of a new tool. Intern J Comput Assist Radiol Surg 8:289–291

29. Mikheev A, Nevsky G, Govindan S et al. (2008) Fully automatic segmentation of the brain from T1-weighted MRI using Bridge Burner algorithm. J Magn Reson Imaging 27:1235–1241. 10.1002/jmri.2f372 [PubMed: 18504741]
30. Jenkinson M, Beckmann CF, Behrens TEJ et al. (2012) FSF Neuroimage 62:782–790. 10.1016/j.neuroimage.2011.09.015
31. Tournier J-D, Smith R, Raffelt D et al. (2019) MRtrix3: a fast, flexible and open software framework for medical image processing and visualisation. Neuroimage 202:116137. 10.1016/j.neuroimage.2019.116137 [PubMed: 31473352]
32. Yu Z, Zhao T, Assländer J et al. (2018) Exploring the sensitivity of magnetic resonance fingerprinting to motion. Magn Reson Imaging 54:241–248. 10.1016/j.mri.2018.09.002 [PubMed: 30193953]
33. Eyres S, Carey A, Gilworth G et al. (2005) Construct validity and reliability of the Rivermead Post-Concussion Symptoms Questionnaire. Clin Rehabil 19:878–887. 10.1191/0269215505cr905oa [PubMed: 16323387]
34. Smith-Seemiller L, Fow NR, Kant R, Franzen MD (2003) Presence of post-concussion syndrome symptoms in patients with chronic pain vs mild traumatic brain injury. Brain Inj 17:199–206. 10.1080/0269905021000030823 [PubMed: 12623496]
35. Giza CC, Hovda DA (2014) The new neurometabolic cascade of concussion. Neurosurgery 75:S24–S33. 10.1227/NEU.0000000000000505 [PubMed: 25232881]
36. Liang D, Bhatta S, Gerzanich V, Simard JM (2007) Cytotoxic edema: mechanisms of pathological cell swelling. Neurosurg Focus 22:1–9. 10.3171/foc.2007.22.5.3
37. Edzes HT, Samulski ET (1977) Cross relaxation and spin diffusion in the proton NMR or hydrated collagen. Nature 265:521–523. 10.1038/265521a0 [PubMed: 834303]
38. Moenninghoff C, Kraff O, Maderwald S et al. (2015) Diffuse axonal injury at ultra-high field MRI. PLoS ONE 10:e0122329. 10.1371/journal.pone.0122329 [PubMed: 25793614]
39. Hütter BO, Altmeppen J, Kraft O et al. (2020) Higher sensitivity for traumatic cerebral microbleeds at 7 T ultra-high field MRI: is it clinically significant for the acute state of the patients and later quality of life? Ther Adv Neurol Disord 13:1–12. 10.1177/1756286420911295
40. Povlishock JT, Katz DI (2005) Update of neuropathology and neurological recovery after traumatic brain injury. J Head Trauma Rehabil 20:76–94. 10.1097/00001199-200501000-00008 [PubMed: 15668572]

Key Points

- In a region-of-interest approach, FA, ADC, and T_1 and T_2 all showed limited utility in differentiating patients from controls at an average of 24 and 90 days post-mild traumatic brain injury.
- T_1 at 24 days, and the serial change in T_1, revealed more and stronger predictive correlations with clinical outcome at 90 days than did T_2, ADC, or FA.
- T_1 showed better prospective identification of non-recovered patients at 90 days than ADC, T_2, and FA.

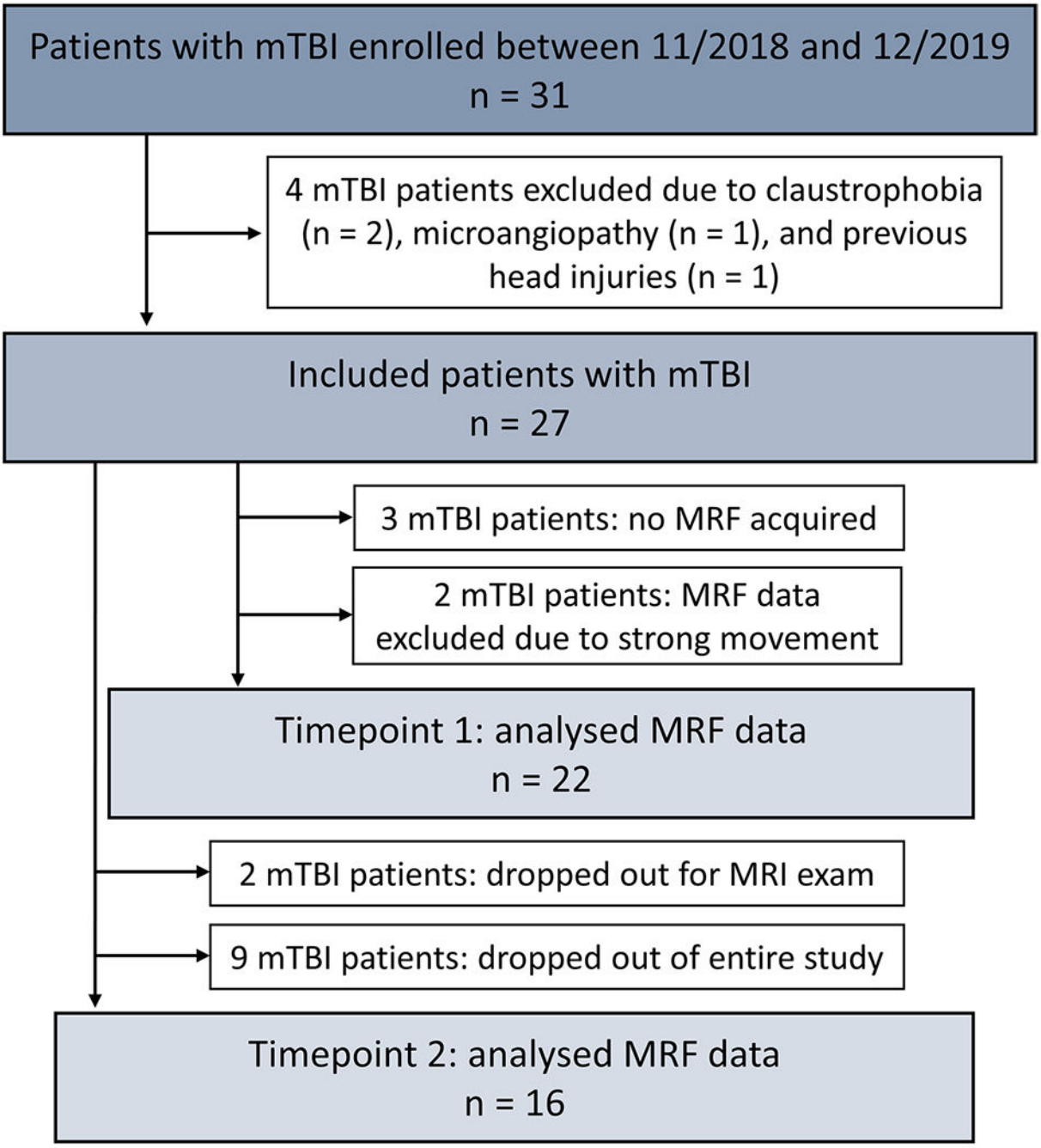

Fig. 1.

Flow diagram of study enrollment. From the initial 31 enrolled patients, four were excluded prior to data acquisition, and five were excluded due to strong movement or missing data, resulting in 22 MRF data sets at timepoint 1. At timepoint 2, two patients declined the MR exam but completed the outcome assessments, and nine patients dropped out of the entire study. mTBI, mild traumatic brain injury; MRF, magnetic resonance fingerprinting

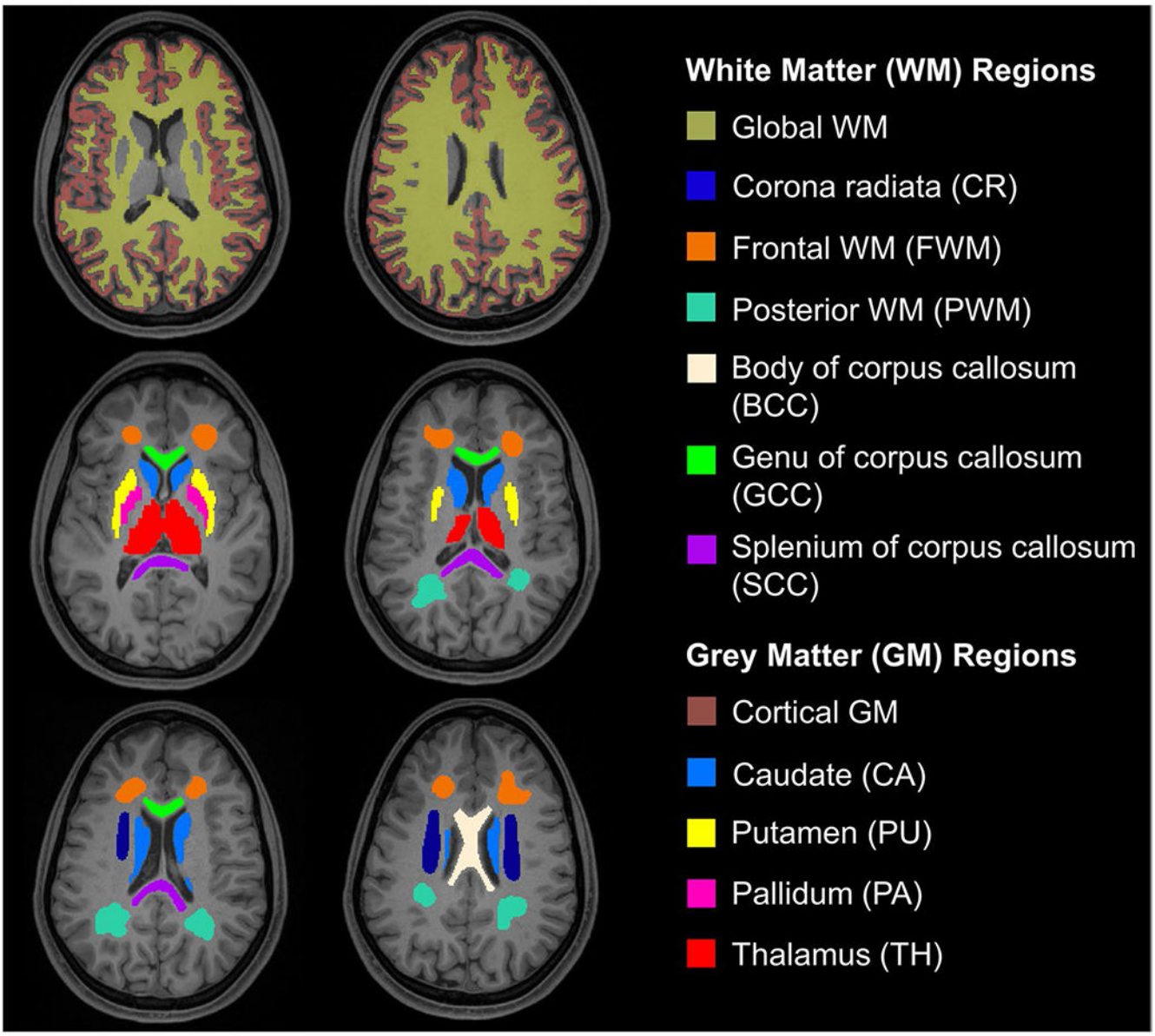

Fig. 2.

Regional analysis of the gray and white matter. T_1-weighted axial MPRAGE images overlaid with the 12 ROIs in which T_1, T_2, FA, and ADC were quantified. Four GM structures (Thalamus, Caudate, Putamen, and Pallidum), global WM, and cortical GM were automatically segmented using FreeSurfer. Six WM regions (Frontal WM, Posterior WM, Corona Radiata, Body of Corpus Callosum, Splenium of Corpus Callosum, and Genu of Corpus Callosum) were manually outlined. The cortical GM and thalamus masks shown have been eroded by one voxel (to reduce CSF contributions)

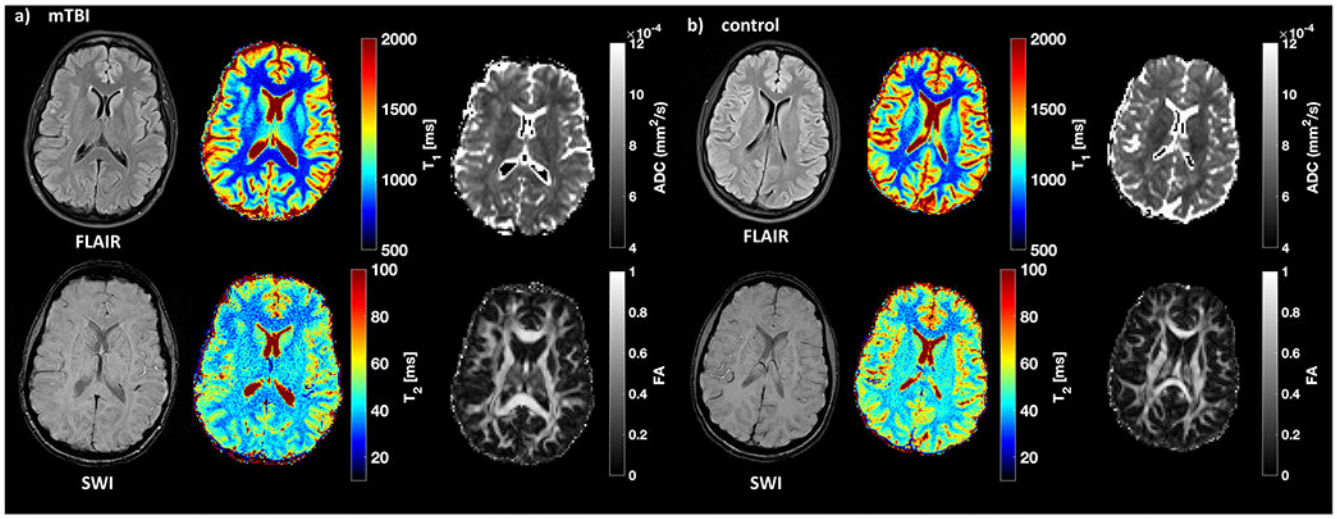

Fig. 3.

Examples of qualitative and quantitative images from a patient with mTBI and a matched control. Fluid-attenuation inversion recovery (FLAIR) and susceptibility-weighted images (SWI) as well as T_1, T_2, ADC, and FA maps from a 34-year-old female patient (**a**) at timepoint 1 and a 30-year-old female (**b**) control. Note the stark T_1 and T_2 difference between gray and white matter

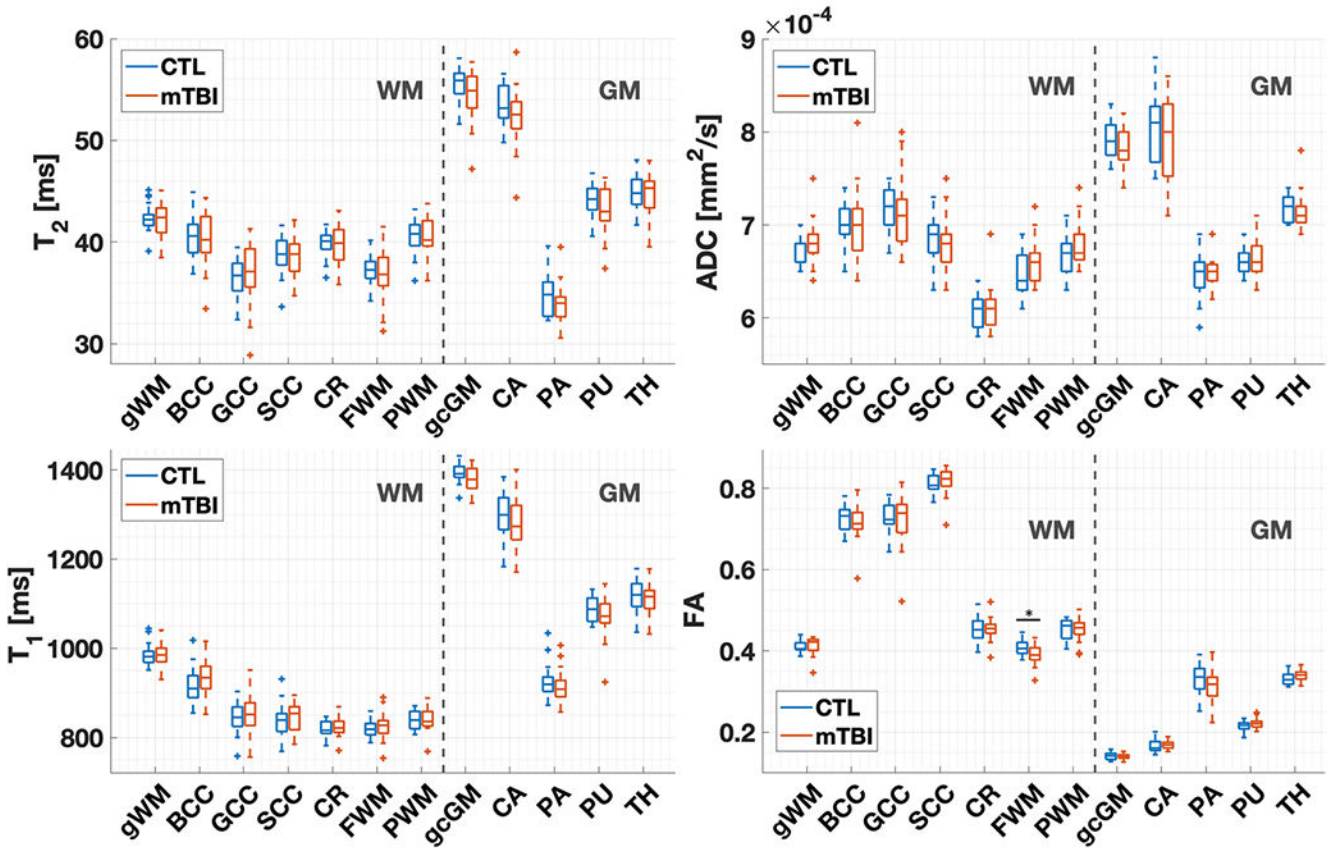

Fig. 4.

T_2, T_1, ADC, and FA distributions in mTBI ($n = 19$) and controls ($n = 18$) (CTL) at timepoint 1. As in the statistical analysis, the boxplots exclude the three non-age-matched patients. Note that T_1 and T_2 in mTBI did not differ from controls for any region. Compared to controls, FA in patients was lower in the frontal white matter (Mann–Whitney test, $p < 0.05$). The middle line in the boxes depicts the median value, and the boxes' top and bottom edges the 25th and 75th percentiles of the data, respectively. The whiskers extend to the most extreme data points not considering outliers (95% of data), which are depicted by a plus sign. BCC body of corpus callosum, SCC splenium of the corpus callosum, GCC genu of the corpus callosum, FWM frontal white matter, PWM posterior white matter, CR corona radiata, CA caudate, PA pallidum, PU putamen, TH thalamus

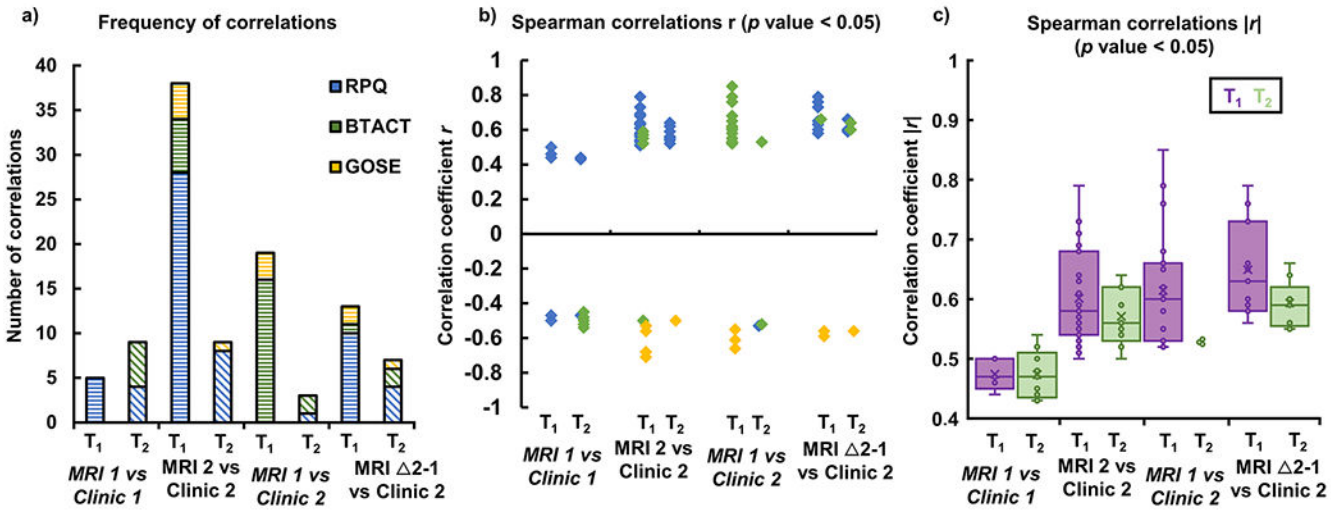

Fig. 5.

Frequency (**a**), directionality (**b**), and strength (**c**) of the correlations between T_1 and T_2 with patient outcome at timepoints 1 and 2. Shown are the statistically significant ($p < 0.05$) T_1 and T_2 Spearman correlations with subtests and/or total scores of the three assessments (RPQ, BTACT, GOSE): cross-sectional associations at timepoint 1 (MRI 1 vs clinic 1) and timepoint 2 (MRI 2 vs clinic 2); and predictive associations for clinical outcome at timepoint 2 of MRI at visit 1 (MRI 1 vs clinic 2), and the change in T_1 and T_2 from timepoint 1 to timepoint 2 (Δ 2–1) (MRI Δ 2–1 vs clinic 2). The associations in (**a**) are plotted with (**b**) the correlation coefficient (*r*) and (**c**) the absolute value of the correlation coefficient (|*r*|) on the y axis. Note that, in general, (*i*) T_1 shows a higher frequency of correlations with clinical outcome, compared to T_2; (*ii*) these correlations are positive for RPQ and BTACT, and negative for GOSE; and (*iii*) they are stronger than those seen for T_2

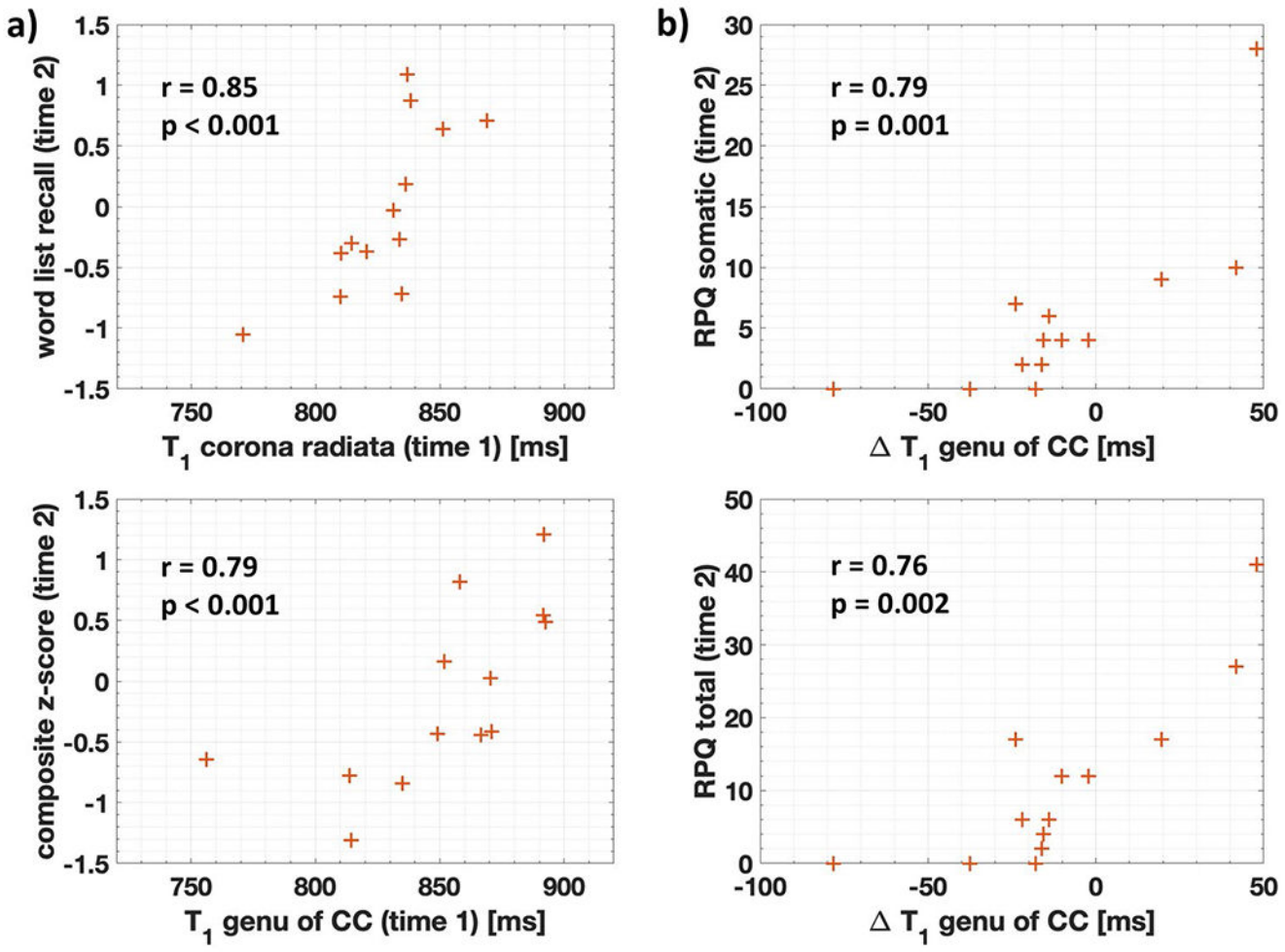

Fig. 6.

Highest predictive correlations with patient outcome at timepoint 2. (**a**) The two highest Spearman correlations *r* (shown with their *p*-values) for the association at timepoint 1 with clinical outcomes at timepoint 2 were found for T_1. (**b**) The two highest Spearman correlations *r* (shown with their *p*-values) for the association of the change from timepoint 1 to timepoint 2 with clinical outcomes at timepoint 2 were also found for T_1. Note that: (*i*) T_1 at timepoint 1 correlates strongly with BTACT, while changes in T_1 from timepoint 1 to timepoint 2 correlate strongly with RPQ; (*ii*) three of the correlations are for genu T_1. CC corpus callosum

Table 1

Demographic and injury characteristics of study participants with mTBI at timepoint 1

Characteristics	mTBI (*n* = 22)	Controls (*n* = 18)
Sex	17 women (77%)/ 5 men (23%)	12 women (67%)/ 6 men (33%)
Age	38 ± 12 y (range: 23—60)	32 ± 18 y (range: 23—54)
MRI findings	WM hyperintensities: 10 (45%) Diffuse axonal injury: 2 (9%) Hemorrhage: 1 (5%)	WM hyperintensities: 6 (33%)
Time after injury (timepoint 1)	24 ± 10 days (range: 8—53)	
Mechanism of injury	Falls: 7 (32%) Pedestrian-object: 5 (23%) Sports/recreation: 3 (14%) Motor vehicle accident: 2 (9%) Other: 5 (22%)	
Loss of consciousness	No: 13 (59%), yes: 6 (27%), unknown: 3 (14%)	
Posttraumatic amnesia	No: 12 (55%), yes: 10 (45%)	
Alteration of consciousness	No: 1 (5%) < 1 min: 3 (14%) 1 – 59 min: 15 (68%) > 1 h: 3 (13%)	

Note. Data in parentheses are either group ranges or percentages. *WM* white matter

Table 2

Summary of patient outcome assessments at timepoints 1 and 2, as well as the change for each measure (value at timepoint 2 minus the value at timepoint 1, Δ 2–1). Only the participants providing data at both time points were included in the change computations. Median, percentage, and range are presented in parentheses. Each *p* value is from the Wilcoxon signed-rank test assessing whether the change was different from zero. The RPQ was analyzed according to different classification methods: RPQ total score (italic bold), RPQ 3 / RPQ 13, and the three-factor model. The BTACT sub-scores are summarized in a composite z-score of cognitive function (italic bold). Note the higher proportion of recovered patients (GOSE), reduction of post-concussion symptoms severity (RPQ), and the improvement of cognitive scores (BTACT) over time

Characteristics			**mTBI timepoint 1 (*n* = 22)**	**mTBI timepoint 2 (*n* = 16)**	**Change (Δ 2–1) (*n* = 13)**
Glasgow Outcome Scale – Extended (GOSE)	5 (lower moderate disability)		1 (5%)	0 (0%)	n/a
	6 (upper moderate disability)		11 (50%)	2 (13%)	n/a
	7 (lower good recovery)		3 (14%)	6 (38%)	n/a
	8 (upper good recovery)		7 (32%)	8 (50%)	n/a
	Average		6.7 ± 1 (6)	7.4 ± 0.7 (7.5)	0.76 ± 0.9 (p = 0.005)
Rivermead Post-Concussion Symptoms Questionnaire (RPQ)	***Total***		21.5 ± 11.9 (0 – 47)	12.1 ± 14 (0 – 46)	−11.12 ± 13.97 (p = 0.007)
	3-factor model	Somatic	11.9 ± 6.9 (0 – 30)	6.4 ± 7.8 (0 – 28)	−6.94 ± 9.26 (p = 0.007)
		Emotional	4.2 ± 14.1 (0 – 15)	2.5 ± 3.8 (0 – 14)	−2.06 ± 3.11 (p = 0.045)
		Cognitive	5.4 ± 3.9 (0 – 12)	3.2 ± 3.5 (0 – 9)	−2.12 ± 3.43 (p = 0.02)
	RPQ 3/13	RPQ 3	3.4 ± 2.5 (0 – 10)	1.4 ± 2.2 (0 – 8)	−2.47 ± 2.43 (p = 0.002)
		RPQ 13	18.1 ± 10.1 (0 – 37)	10.9 ± 12.8 (0 – 42)	−8.41 ± 12.65 (p = 0.009)
Brief Test of Adult Cognition by Telephone (BTACT)	***BTACT composite z-score***	−0.38 ± 0.67 (−1.44 – 0.86)	−0.08 ± 0.77 (−1.31 – 1.47)	0.43 ± 0.45 (p = 0.001)	n/a
	Subtest z-scores	Word list recall	−0.52 ± 1.07 (−2.67 – 2.06)	0.0 ± 0.85 (−1.13 – 1.77)	0.58 ± 0.81 (p = 0.005)
		Short – delay word list recall	−0.60 ± 0.79 (−1.75 – 0.76)	−0.18 ± 0.95 (−1.77 – 1.78)	0.27 ± 0.79 (p = 0.1637)
		Backward digit	−0.11 ± 0.90 (−1.39 – 1.64)	−0.17 ± 1.04 (−2.15 – 1.68)	0.17 ± 0.71 (p = 0.65)
		Category fluency	0.0 ± 1.27 (−1.87 – 2.92)	−0.02 ± 1.07 (−2.07 – 1.95)	0.04 ± 0.69 (p = 0.723)
		Number series	−0.70 ± 1.52 (−3.74 – 1.36)	−0.08 ± 1.02 (−1.79 – 1.65)	0.9 ± 1.03 (p = 0.005)
		Backward counting	−0.46 ± 0.91 (−2.05 – 1.95)	−0.05 ± 1.77 (−2.86 – 4.30)	0.78 ± 1.61 (p = 0.052)

Note. *n/a* not applicable

Table 3

The mean, standard deviation (SD), median, and interquartile range (IQR) of the within-subject change in MRI measures among mTBI patients. The change was computed for each subject as the value at timepoint 2 minus the value at timepoint 1. Only patients providing data at both times were included in the computations. *p*-values are from the matched-pair Wilcoxon signed-rank test (WSRT) assessing whether the change was different from zero. Only measures with $p < 0.05$ are presented

Measure	Region	Change (Δ 2–1)				WSRT
		Mean	SD	Median	IQR	*p* value
FA	Body of corpus callosum	−0.039	0.095	−0.018	0.047	0.019
	Corona radiata	−0.008	0.014	−0.01	0.017	0.020
	Thalamus	−0.006	0.006	−0.004	0.009	0.004
	Global cortical GM	−0.013	0.028	−0.005	0.014	0.014
T_2 (ms)	Pallidum	1.7	5.1	0.7	0.7	0.025

Table 4

MRI measures at timepoint 1, and within-subject change in MRI measures, with the highest utility for predicting timepoint 2 recovered and non-recovered status as assessed by GOSE. The *p* values from the logistic regression and the area under the receiver operating characteristic curve (AUC) to assess the utility of imaging measure at timepoint 1 and of the within-subject change as a predictor of recovery at timepoint 2 are presented, followed by the mean and standard deviation (SD) of both groups and *p* values from the Mann–Whitney (MW) test. Only measures in regions with an AUC ≥0.80 are presented

Measure	**Region**	**Logistic regression *p* value**	**AUC**	**No recovery (*n* = 8)**		**Recovery (*n* = 11)**		**MW *p* value**
				Mean	SD	Mean	SD	
ADC (mm^2/s)	Corona radiata	0.049	0.80	0.62	0.01	0.6	0.01	0.023
T_1 (ms)	Corona radiata	0.123	0.80	837	18	817	023	0.063
	Posterior WM	0.067	0.83	859	19	831	026	0.035
	Splenium of corpus callosum	0.04	0.88	864	26	822	025	0.018
Change (Δ 2–1) in T_1 (ms)	Frontal WM	0.135	0.81	0.116	0.138	−0.122	0.268	0.074
	Genu of corpus callosum	0.176	0.83	0.113	0.3	−0.28	0.238	0.051